

A HIDDEN MARKOV MODEL FOR STATISTICAL ARBITRAGE IN INTERNATIONAL CRUDE OIL FUTURES MARKETS

VIVIANA FANELLI, CLAUDIO FONTANA, AND FRANCESCO ROTONDI

ABSTRACT. We study statistical arbitrage strategies in international crude oil futures markets. We analyse strategies that extend classical pairs trading strategies, considering two benchmark crude oil futures (Brent and WTI) together with the recently introduced Shanghai crude oil futures. We show that the time series of these three futures prices are cointegrated and we introduce a mean-reverting regime-switching process modulated by a hidden Markov chain to model the cointegration spread. By relying on this model and applying online filter-based parameter estimators, we implement and test several statistical arbitrage strategies. Our analysis reveals that statistical arbitrage strategies involving the recently introduced Shanghai futures are profitable even under conservative levels of transaction costs and over different time periods. Statistical arbitrage strategies involving only two of these three futures contracts or the three traditional crude oil futures (Brent, WTI, Dubai) deliver a lower investment performance.

1. INTRODUCTION

Pairs trading strategies represent a well-known instance of statistical arbitrage strategies that exploit temporary deviations in the prices of similar securities from their long-term equilibrium in order to achieve profits when convergence to the equilibrium is reached (see, e.g., [?], [?], [?]). Since one cannot determine *ex ante* when prices are going to realign, such strategies do not constitute pure arbitrage opportunities but rather statistical arbitrage opportunities, that are expected to deliver a profit over a sufficiently long time horizon. The profitability of this type of strategies requires a strong long-term relationship, so that mispricings are temporary and likely to revert back quickly. This is typically captured through the existence of a cointegration relation among the considered security prices.

In this work, we study statistical arbitrage strategies in international crude oil futures markets, inspired by pairs trading strategies. The futures contracts we consider are two established benchmark crude oil futures, the Brent and the West Texas Intermediate (WTI), together with the Shanghai crude oil futures more recently introduced in 2018¹. It is known that the Brent and the WTI futures prices are cointegrated (see, e.g., [?], [?], [?], [?]), while preliminary evidence (see [?]) shows that the recently introduced Shanghai crude oil futures tends to cointegrate with

Date: September 20, 2024.

Key words and phrases. Pairs trading; crude oil futures; cointegration; spread process; mean-reverting process; regime switching; stochastic filtering; EM algorithm.

JEL classification. C51, C58, G11, G15.

Financial support from the University of Padova (research programme STARS StG PRISMA - “Probabilistic Methods for Information in Security Markets”) is gratefully acknowledged. This work is supported by the project P20224TM7Z (subject area: PE - Physical Sciences and Engineering) “Probabilistic methods for energy transition” funded by the European Union - Next Generation EU under the National Recovery and Resilience Plan, Mission 4 Component 1 CUP C53D23008390001.

Corresponding author: F. Rotondi.

¹The Shanghai International Energy Exchange (INE) introduced crude oil futures on March 26, 2018. These contracts are known as the *Shanghai crude oil futures* and are traded on the Shanghai Futures Exchange (SHFE). They are quoted in Chinese yuan and based on the INE’s own benchmark, which is a blend of various Middle Eastern and Asian crude oil grades that reflects the specific needs of China’s oil imports.

them as well. These empirical findings suggest the possibility of achieving statistical arbitrage opportunities when these three crude oil futures are jointly traded. This represents the starting point and the motivation of this work.

We examine whether the introduction of the Shanghai crude oil futures has enabled international arbitrageurs to achieve profitable investments through statistical arbitrage strategies. Pairs trading on traditional crude oil benchmarks has already been studied (see, e.g., [?], [?], [?]), while [?] test pairs trading strategies on the different Shanghai futures contracts traded at the INE. To the best of our knowledge, our work is the first to consider statistical arbitrage strategies involving simultaneously more than two futures contracts and, in particular, the established crude oil futures together with the recently introduced Shanghai crude oil futures.

From a methodological viewpoint, we improve on existing approaches to pairs trading by assessing the cointegration among the three futures prices at the same time and modelling the resulting cointegration spread by a mean-reverting process with regime-switching modulated by a hidden Markov chain. This generalizes the approach of [?] and [?] and enables us to capture time-varying cointegration regimes. As the Markov chain is unobserved, we employ stochastic filtering techniques to estimate the current regime and the model parameters, similarly as in [?] and [?]. Parameter estimation is done by means of a filter-based version of the Expectation Maximization (EM) algorithm, as introduced in [?] (see also [?] for an application to credit risk). The filtering approach enables us to estimate the most likely regime and the model parameters in a dynamic way, thereby ensuring that the model stays constantly tuned to the actual market situation. In turn, this will enable us to construct statistical arbitrage strategies that are dynamically updated as new information arrives. After estimating our model over a training sample, we move out-of-sample and analyse several types of statistical arbitrage strategies.

Our empirical analysis shows that statistical arbitrage strategies involving the three futures (Brent, WTI and Shanghai) at the same time, rather than just two of them, deliver significant investment performances even when transaction costs are accounted for. Moreover, strategies that exploit our hidden Markov model for the cointegration spread are remarkably profitable when compared to more traditional strategies based only on time series features. We find that the investment performances of these strategies are significantly reduced if the Shanghai futures is replaced by another standard crude oil benchmark as the Dubai crude oil futures. Our findings indicate that the greater profitability of statistical arbitrage strategies involving the Shanghai futures can be explained by the higher speed of adjustment of the Shanghai futures prices compared to the Brent and the WTI. This implies that the Shanghai futures prices tend to revert back quickly to the long-run relationship, making easier the exploitation of temporary mispricings. This finding is in line with the fact that the profitability of statistical arbitrage strategies tends to decline over time as markets develop (see, e.g., [?]), while the introduction of a new security can represent a valuable opportunity for arbitrageurs².

The contribution of the paper is threefold. First, we corroborate the evidence of cointegration among the recently introduced Shanghai crude oil futures and two long-standing crude oil futures benchmarks, the Brent and the WTI. To our knowledge, this is the first time that cointegration is assessed considering these three contracts together, rather than on a pairwise basis. As a second contribution, we propose a mean-reverting stochastic model for the cointegration spread that allows for regime switching by means of a hidden Markov chain determining the parameters

²See for instance [?] for an analysis of arbitrage opportunities in the emerging markets for cryptocurrencies.

of the process. We apply filtering techniques to dynamically estimate the most likely regime and the model parameters. Finally, we empirically analyze different statistical arbitrage strategies involving three crude oil futures contracts. Our results indicate that strategies that include a newly introduced security, like the Shanghai crude oil futures, along with traditional and well-established ones, like the Brent and the WTI, are remarkably profitable and robust.

The paper is structured as follows. Section 2 describes the cointegration structure and the stochastic model for the cointegration spread. Section 3 describes the statistical arbitrage strategies we implement and how their performance is assessed. Section 4 contains the results of our empirical analysis, while Section 5 concludes. The results of an additional empirical analysis based on daily data are reported as Supplementary Material.

2. COINTEGRATION ANALYSIS AND SPREAD MODELLING

In this section, we introduce the stochastic model for the long-run relationship among the three crude oil future prices (Section 2.1) and describe how the model parameters can be dynamically estimated by means of filtering techniques combined with the EM algorithm (Section 2.2).

2.1. A mean-reverting hidden Markov model. Let $F^i = (F_t^i)_{t \geq 0}$ denote the futures price process³, for $i \in \{B, S, W\}$, of the Brent (B), the Shanghai (S) and the WTI futures (W). The processes F^B and F^W are typically found to be cointegrated, as documented by [?] and [?] among others. Similarly, [?] and [?] show that F^S is cointegrated with F^B and with F^W . Therefore, it is reasonable to guess that the three futures price processes jointly considered are cointegrated, similarly to the case of the Brent, the Dubai and the WTI futures prices (see [?]). The cointegration among F^B , F^S , F^W has not been tested in previous works and will be shown to hold in the following. In the presence of cointegration, there exists a linear combination of F^B , F^S , F^W that follows a stationary and possibly mean-reverting process. As usual in cointegration analysis, we call this linear combination the *spread process* and denote it by $S = (S_t)_{t \geq 0}$. More specifically,

$$(2.1) \quad S_t := \lambda^0 + \sum_{i=B,S,W} \lambda^i F_t^i,$$

for suitable coefficients $\lambda^0, \lambda^B, \lambda^S, \lambda^W$ that constitute the *cointegration vector* λ .

Using the cointegration vector estimated in-sample an investor can evaluate the spread out-of-sample and set up statistical arbitrage strategies based on it, taking as portfolio weights the elements of the cointegration vector. These strategies turn out to be profitable as long as the cointegrating relationship is stable, namely as long as the spread S is stationary. In a standard cointegration analysis, the cointegration vector λ is assumed to be constant. However, previous works on the Brent (see, e.g., [?]) and on the WTI document the existence of structural breaks in the cointegration vector (see, e.g., [?]), showing also that the cointegration vector depends significantly on the time window over which the relationship is estimated. As already noticed by [?], this might severely impact pairs trading strategies based on cointegration. It is therefore appropriate to model the spread as a stochastic process with regime switching, updating the model parameters dynamically by incorporating new information as soon as it becomes available. In this work, we shall adopt this approach, starting from the explicit modelling of the spread process.

³We consider statistical arbitrage strategies based on the price processes of several assets. We refer to [?] for an analysis of statistical arbitrage opportunities based on asset returns rather than prices.

Let $(\Omega, \mathcal{F}, \mathbb{F} = (\mathcal{F}_t)_{t \geq 0}, \mathbb{P})$ be a filtered probability space supporting a Brownian motion $W = (W_t)_{t \geq 0}$ and a Markov chain $\mathbf{X} = (\mathbf{X}_t)_{t \geq 0}$ with N states and transition matrix $\mathbf{\Pi}$. The states of the Markov chain \mathbf{X} represent different market regimes, thus capturing the time-varying nature of the cointegrating relationship. The Markov chain \mathbf{X} admits a semimartingale representation of the form

$$\mathbf{X}_t = \mathbf{X}_0 + \int_0^t \mathbf{\Pi} \mathbf{X}_s ds + \mathbf{M}_t,$$

where $\mathbf{M} = (\mathbf{M}_t)_{t \geq 0}$ is a martingale with $\mathbf{M}_0 = 0$ (see [?], Chapter 7).

For the spread process S , we assume mean-reverting dynamics with regime switching:

$$(2.2) \quad dS_t = a(\mathbf{X}_t) (\beta(\mathbf{X}_t) - S_t) dt + \xi(\mathbf{X}_t) dW_t, \quad \text{with } S_0 = s_0 \in \mathbb{R},$$

where α, β, ξ are real-valued functions on \mathbb{R}^N . Without loss of generality and similarly as in [?], we assume that the state space of the Markov chain \mathbf{X} is the canonical basis of \mathbb{R}^N , denoted by $\{\mathbf{e}_1, \dots, \mathbf{e}_N\}$, so that $a(\mathbf{X}_t) = \mathbf{a}^\top \mathbf{X}_t$ with $\mathbf{a} \in \mathbb{R}^N$. For each $i = 1, \dots, N$, the component a_i represents the speed of mean-reversion of S in the i^{th} regime. Analogously, β_i (resp. ξ_i) represents the long-run mean (resp. volatility) of S in the i^{th} regime. The resulting model for S is a OrnsteinUhlenbeck process driven by a hidden Markov model (OU-HMM henceforth) which has been used in the literature for the modelling of interest rates ([?], [?]), commodity spot prices ([?]) and spreads between equity price processes ([?]).

Since the current market regime is generally unknown by market participants, we assume that the Markov chain \mathbf{X} is unobservable. As a consequence, the current state of \mathbf{X} has to be filtered from the observations of the spread. Since we want to implement statistical arbitrage strategies that exploit the probabilistic structure of the model (2.2) for S , we need to estimate \mathbf{a}, β, ξ and the transition matrix $\mathbf{\Pi}$. In this partial observation setup, the estimation of \mathbf{a}, β, ξ and $\mathbf{\Pi}$ can be done by a filter-based Expectation Maximization algorithm that we now describe.

2.2. The filter-based Expectation Maximization algorithm. We now describe the filter-based Expectation Maximization (EM) algorithm for the estimation of the OU-HMM in (2.2). The following results are adapted from the general techniques described in [?] and specifically applied to an Ornstein-Uhlenbeck process in [?].

As a first step, we discretize the continuous-time model (2.2). This discretization is needed not only because only discrete observations of S are available in practice, but also because in a continuous-time setting the EM algorithm does not allow to estimate ξ , since it is based on equivalent measure transformations and volatility cannot be changed under equivalent measures.

Consider the spread process S over a time interval $[t, t + \Delta]$, with Δ denoting the time step. If \mathbf{X} is constant over this interval, we can write explicitly the solution of (2.2) as

$$S_{t+\Delta} = e^{-a(\mathbf{X}_t)\Delta} S_t + \beta(\mathbf{X}_t)(1 - e^{-a(\mathbf{X}_t)\Delta}) + \xi(\mathbf{X}_t) \int_t^{t+\Delta} e^{-a(\mathbf{X}_t)(t+\Delta-s)} dW_s.$$

From this equation we derive the discrete-time version $y = (y_t)_{t \in \mathbb{N}}$ of the spread:

$$(2.3) \quad y_{t+1} = \gamma(\mathbf{X}_t) + \alpha(\mathbf{X}_t) y_t + \eta(\mathbf{X}_t) z_t,$$

where $(z_t)_{t \in \mathbb{N}}$ is a sequence of i.i.d. standard normal random variables and

$$(2.4) \quad \begin{aligned} \alpha(\mathbf{X}_t) &:= e^{-a(\mathbf{X}_t)\Delta}, \\ \gamma(\mathbf{X}_t) &:= \beta(\mathbf{X}_t) (1 - e^{-a(\mathbf{X}_t)\Delta}), \\ \eta(\mathbf{X}_t) &:= \xi(\mathbf{X}_t) \sqrt{\frac{1 - e^{-2a(\mathbf{X}_t)\Delta}}{2a(\mathbf{X}_t)}}. \end{aligned}$$

Analogously, we consider a discrete-time version of the Markov chain \mathbf{X} as

$$\mathbf{X}_{t+1} = \mathbf{\Pi}\mathbf{X}_t + \mathbf{v}_{t+1},$$

with \mathbf{v}_{t+1} denoting a martingale increment. We also introduce the following auxiliary quantities that will be needed for the recursive estimation of the model parameters:

- $J_t^{ij} := \sum_{n=1}^t \langle \mathbf{X}_{n-1}, \mathbf{e}_i \rangle \langle \mathbf{X}_n, \mathbf{e}_j \rangle$, representing the cumulative number of jumps of \mathbf{X} from state \mathbf{e}_i to state \mathbf{e}_j until time t .
- $O_t^i := \sum_{n=1}^t \langle \mathbf{X}_n, \mathbf{e}_i \rangle$, representing the occupation time of \mathbf{X} in state \mathbf{e}_i until time t .
- $T_t^i(f) = \sum_{n=1}^t \langle \mathbf{X}_{n-1}, \mathbf{e}_i \rangle f_n$, where f_n is a generic function of the observations of y up to time n (in our case, the function f_n will be given by $f_n = y_n$, $f_n = y_n^2$ or $f_n = y_n y_{n-1}$).

We denote by $\mathbb{F}^y = (\mathcal{F}_t^y)_{t \in \mathbb{N}}$, with $\mathcal{F}_t^y := \sigma\{y_0, \dots, y_t\}$ for all $t \in \mathbb{N}$, the filtration generated by the process y . We assume that \mathbb{F}^y represents the information available to the investor, who cannot observe the Markov chain \mathbf{X} and can only access discrete-time observations of the spread.

We now state the recursive filtering equations for the unobserved Markov chain \mathbf{X} and the quantities J, O, T , from which we derive the recursive equations for the EM estimators of $\boldsymbol{\alpha}, \boldsymbol{\gamma}, \boldsymbol{\eta}$ and $\mathbf{\Pi}$. For $t \in \mathbb{N}$, we denote by $\hat{\mathbf{X}}_t := \mathbb{E}[\mathbf{X}_t | \mathcal{F}_t^y]$ the filtered estimate of the latent Markov chain at time t on the basis of the information generated by the observation process y up to time t . In an analogous way we define the filtered estimates $\hat{J}_t^{ij}, \hat{O}_t^i$ and $\hat{T}_t^i(f)$ of the quantities introduced above. Moreover, we denote by $\hat{\boldsymbol{\alpha}}^{(t)} = (\hat{\alpha}_i^{(t)})_{i=1, \dots, N}$ the estimate of the parameter $\boldsymbol{\alpha}$ on the basis of the information generated by the observation process y up to time t . The quantities $\hat{\boldsymbol{\gamma}}^{(t)}, \hat{\boldsymbol{\eta}}^{(t)}, \hat{\mathbf{\Pi}}^{(t)}$ are defined analogously.

As explained in [?, Chapter 8], in order to filter the unobserved Markov chain \mathbf{X} one can resort to a change of measure passing from \mathbb{P} to an equivalent probability measure $\tilde{\mathbb{P}}$ under which the observation process y is independent of the Markov chain \mathbf{X} . For each $T \in \mathbb{N}$, the probability measures \mathbb{P} and $\tilde{\mathbb{P}}$ are related by the Radon-Nikodym derivative

$$\Lambda_T = \frac{d\tilde{\mathbb{P}}}{d\mathbb{P}} \Big|_{\mathcal{F}_T} = \prod_{t=1}^T \lambda_t,$$

where

$$(2.5) \quad \lambda_t = \frac{1}{\eta(\mathbf{X}_{t-1})} \exp \left(-\frac{1}{2} \left(\frac{(y_t - y_{t-1}\alpha(\mathbf{X}_{t-1}) - \gamma(\mathbf{X}_{t-1}))^2}{\eta(\mathbf{X}_{t-1})^2} - y_t^2 \right) \right),$$

with $\Lambda_0 = 1$. For convenience of notation, it is useful to represent the possible values of λ_t in (2.5) associated to each of the N states of \mathbf{X} by a diagonal matrix $\mathbf{D}_t = [d_t^{ij}]_{i,j=1, \dots, N}$ with

$$(2.6) \quad d_t^{ii} = \frac{1}{\eta_i} \exp \left(-\frac{1}{2} \left(\frac{(y_t - y_{t-1}\alpha_i - \gamma_i)^2}{\eta_i^2} - y_t^2 \right) \right), \quad \text{for } i = 1, \dots, N.$$

The starting point of the filtering algorithm is a set of initial guesses for the quantities \mathbf{X}_0 (that delivers also the initial values of the O_0^i 's) and for $\mathbf{\Pi}, \boldsymbol{\gamma}, \boldsymbol{\alpha}, \boldsymbol{\eta}$.

By performing similar computations as in [?], the recursive filtering equations for \mathbf{X} and for the auxiliary quantities J, O, T are given as follows:

$$(2.7) \quad \begin{aligned} \hat{\mathbf{X}}_{t+1} &= \mathbf{\Pi} \mathbf{D}_{t+1} \hat{\mathbf{X}}_t, \\ \hat{J}_{t+1}^{i,j} &= \langle \mathbf{1}, \mathbf{\Pi} \mathbf{D}_{t+1} \hat{J}_t^{i,j} + \langle \hat{\mathbf{X}}_t, \mathbf{e}_i \rangle \langle \mathbf{D}_{t+1} \mathbf{e}_i, \mathbf{e}_j \rangle \pi_{ij} \mathbf{e}_j \rangle, \\ \hat{O}_{t+1}^i &= \langle \mathbf{1}, \mathbf{\Pi} \mathbf{D}_{t+1} \hat{O}_t^i + \langle \hat{\mathbf{X}}_t, \mathbf{e}_i \rangle \langle \mathbf{D}_{t+1} \mathbf{e}_i, \mathbf{e}_i \rangle \mathbf{\Pi} \mathbf{e}_i \rangle, \\ \hat{T}_{t+1}^i(f) &= \langle \mathbf{1}, \mathbf{\Pi} \mathbf{D}_{t+1} \hat{T}_t^i(f) + \langle \hat{\mathbf{X}}_t, \mathbf{e}_i \rangle \langle \mathbf{D}_{t+1} \mathbf{e}_i, \mathbf{e}_i \rangle f_t \mathbf{\Pi} \mathbf{e}_i \rangle, \end{aligned}$$

for all $t \in \mathbb{N}$, where we denote by $\mathbf{1}$ the unit vector in \mathbb{R}^N . Observe that the filters in (2.7) depend on $\mathbf{\Pi}$ and, through the matrix \mathbf{D}_{t+1} , also on $\boldsymbol{\gamma}, \boldsymbol{\alpha}, \boldsymbol{\eta}$. Therefore, when implementing the filtering procedure in practice these quantities must be replaced by their estimates $\hat{\mathbf{\Pi}}^{(t)}, \hat{\boldsymbol{\gamma}}^{(t)}, \hat{\boldsymbol{\alpha}}^{(t)}, \hat{\boldsymbol{\eta}}^{(t)}$ obtained at the previous time point t . In analogy to [?], the equations for the EM recursive estimates of $\mathbf{\Pi}, \boldsymbol{\gamma}, \boldsymbol{\alpha}, \boldsymbol{\eta}$ at time t are given by

$$\begin{aligned}
 \hat{\pi}_{ij}^{(t+1)} &= \frac{\hat{J}_{t+1}^{i,j}}{\hat{O}_{t+1}^j}, \\
 \hat{\gamma}_i^{(t+1)} &= \frac{\hat{T}_{t+1}^i(y_{t+1}) - \hat{\alpha}_i^{(t)} \hat{T}_t^i(y_t)}{\hat{O}_{t+1}^i}, \\
 \hat{\alpha}_i^{(t+1)} &= \frac{\hat{T}_t^i(y_{t+1}, y_t) - \hat{\gamma}_i^{(t+1)} \hat{T}_t^i(y_t)}{\hat{T}_t^i(y_t^2)}, \\
 \hat{\eta}_i^{(t+1)} &= \frac{\hat{T}_{t+1}^i(y_{t+1}^2) + (\hat{\alpha}_i^{(t+1)})^2 \hat{T}_t^i(y_t^2) + (\hat{\gamma}_i^{(t+1)})^2 \hat{O}_{t+1}^i}{\hat{T}_t^i(y_t^2)} \\
 &\quad + \frac{\hat{\gamma}_i^{(t+1)} \hat{T}_{t+1}^i(y_{t+1}) - 2\hat{\alpha}_i^{(t+1)} \hat{T}_t^i(y_{t+1}, y_t) - 2\hat{\alpha}_i^{(t+1)} \hat{\gamma}_i^{(t+1)} \hat{T}_t^i(y_t)}{\hat{O}_{t+1}^i}.
 \end{aligned} \tag{2.8}$$

It is worth noting that every time a new observation becomes available all the filters in (2.7) and (2.8) are simply updated without re-running the whole filtering algorithm, due to its recursive nature. This is an advantage of the online filter-based EM algorithm, which allows the model to be constantly tuned to the actual market information in a computationally efficient way.

Remark 2.1 (Numerical aspects). In this remark we address some numerical aspects that arise when implementing the above filtering algorithm in practice:

- (1) As far as the initialization of the algorithm is concerned, the initial state of the Markov chain \mathbf{X}_0 also determines O_0^i . In our analysis we set $\hat{\mathbf{X}}_0 = \mathbf{e}_1$ by convention. This implies $\hat{O}_0^1 = 1$ and $\hat{O}_0^i = 0$ for $i = 2, \dots, N$. With respect to the initial guess for $\mathbf{\Pi}$, if $N = 2$, we set $\hat{\pi}_{11}^{(0)} = 0.6$ and $\hat{\pi}_{22}^{(0)} = 0.5$ since the perfectly symmetric initial guess $\hat{\pi}_{11}^{(0)} = \hat{\pi}_{22}^{(0)} = 0.5$ tends to create numerical instabilities as there is no difference across states in the transition matrix. If $N = 3$, we set $\hat{\pi}_{11}^{(0)} = 0.5, \hat{\pi}_{12}^{(0)} = 0.25, \hat{\pi}_{21}^{(0)} = 0.3, \hat{\pi}_{22}^{(0)} = 0.4$ and $\hat{\pi}_{31}^{(0)} = 0.2, \hat{\pi}_{33}^{(0)} = 0.6$. The initial guesses for $\boldsymbol{\gamma}, \boldsymbol{\alpha}$ and $\boldsymbol{\eta}$ are derived from the data. More specifically, if the Markov chain \mathbf{X} was constant, then the process y would follow a simple AR(1) process with constant parameters satisfying

$$(2.9) \quad y_{t+1} = \gamma + \alpha y_t + \varepsilon_{t+1},$$

where $\varepsilon = (\varepsilon_t)_{t \in \mathbb{N}}$ is a Gaussian white noise process with variance η^2 . In this case, the parameters γ, α, η could be estimated by ordinary least squares. In our empirical analysis we do so using the first 20 datapoints of y , corresponding to one month of daily observations (this is twice the batch parameter m introduced below and that we set equal to 10). For $N = 1$ we therefore set $\hat{\gamma}^{(0)} = \hat{\gamma}_{\text{OLS}}, \hat{\alpha}^{(0)} = \hat{\alpha}_{\text{OLS}}$ and $\hat{\eta}^{(0)} = \hat{\eta}_{\text{OLS}}$, where $\hat{\gamma}_{\text{OLS}}, \hat{\alpha}_{\text{OLS}}$ and $\hat{\eta}_{\text{OLS}}$ denote the ordinary least square estimates of the parameters of (2.9). For $N = 2$ we let the initial guess for the two states for all the parameters be equally spaced with respect to the OLS estimates determined as above. Hence, we set $\hat{\gamma}_1^{(0)} = 1.3\hat{\gamma}_{\text{OLS}}$ and $\hat{\gamma}_2^{(0)} = 0.7\hat{\gamma}_{\text{OLS}}$, and analogously for the other two parameters. For $N = 3$ we follow the same reasoning and set $\hat{\gamma}_1^{(0)} = 1.3\hat{\gamma}_{\text{OLS}}, \hat{\gamma}_2^{(0)} = \hat{\gamma}_{\text{OLS}}$ and $\hat{\gamma}_3^{(0)} = 0.7\hat{\gamma}_{\text{OLS}}$, and analogously for the remaining parameters. We point out that the EM algorithm is robust with respect to the specification of the initial guesses.

- (2) During the first iterations of the algorithm it might happen that the quantity \hat{O}_{t+1}^i , which appears at the denominator in $\hat{\gamma}_i^{(t+1)}$ and $\hat{\eta}_i^{(t+1)}$ in (2.8), is equal to zero. This happens if the Markov chain has never visited state i before time $t + 1$. In this case, there is no way to update $\hat{\gamma}_i^{(t+1)}$ and $\hat{\eta}_i^{(t+1)}$, which are left unchanged throughout the current iteration of the algorithm.
- (3) Quantities like $\hat{T}_t^i(y_{t-1}^2)$, appearing at the denominator in $\hat{\alpha}_i^{(t+1)}$ and $\hat{\eta}_i^{(t+1)}$ in (2.8), might take very small values (especially when the y 's are close to zero) and this might induce numerical instabilities. The same issue can arise when computing the diagonal elements of \mathbf{D} if the $\hat{\eta}_i^{(t+1)}$'s are too close to zero. If not controlled for, these instabilities propagate, preventing the algorithm to converge. Therefore, for all denominators in (2.8) we check that the new estimate of the quantity of interest is not smaller/larger than ten times the previous estimate and, in case, we truncate the new estimate to that level.
- (4) The two previous issues can be mitigated by adopting a *batchwise* approach, as pointed out in [?], updating the parameters in (2.8) not at every time point t as the filters in (2.7) but rather every m steps. This technique stabilizes the estimates of the filtered quantities in (2.7) and, as a consequence, the parameter estimates in (2.8). In our analysis we set $m = 10$, which in practice amounts to update the model parameters every two weeks.

3. STATISTICAL ARBITRAGE STRATEGIES

In this section we introduce several statistical arbitrage strategies that shall be tested on data (Section 3.1) and describe the performance measures used to assess their profitability (Section 3.2).

3.1. Statistical arbitrage strategies. As explained in [?, Chapter 8], the basic intuition behind pairs trading is that whenever the spread deviates “sufficiently” from its equilibrium value, the investor should open a trading position, appropriately investing in the underlying assets. The position is then closed when this deviation corrects itself and the spread reverts to its equilibrium value. The precise specification of what we mean above by “sufficiently” determines a specific trading strategy, which can be summarized by a simple rule based on *opening* and *closing* signals.

Regardless of the specification of opening/closing signals, we assume that the trading position is determined by the cointegration vector $\lambda = (\lambda^0, \lambda^B, \lambda^S, \lambda^W)$ in (2.1), where λ^0 determines the borrowing/lending of money from a riskless money market account (earning zero interest rate, for simplicity of presentation). Abstracting from transaction costs, if an opening signal is received at time t when $S_t > 0$ (resp. $S_t < 0$), the investor has to go short (resp. long) on portfolio λ . This generates an inflow of money at time t equal to $|S_t|$. Closing this position when the spread reverts back to zero will deliver no cashflow. Therefore, these strategies are designed to deliver positive payoffs at their opening, with zero cashflows when they are closed, similarly to arbitrage opportunities of the second kind (see, e.g., [?]). However, since it is not known ex ante if and when S_t will revert back to zero, these strategies are not pure arbitrage opportunities but rather statistical arbitrage opportunities (see [?] and [?] for a mathematical formalization of the concept of statistical arbitrage).

In our analysis we consider five different statistical arbitrage strategies. The first one is a simple benchmark and requires no explicit modelling of the spread process. The second and the fourth strategies rely only on sample estimates of the moments of the spread. On the contrary, the third and the fifth strategies exploit our stochastic model for the spread, as they are based

on the one-step ahead forecast of the spread and on its forecast interval. While the timing of opening signals differs across the five different rules, the closing one is assumed to be the same for simplicity of comparison. In particular, if there was an open position at time $t - 1$, the position is closed at time t if the spread S_t changes sign (in discrete time, this corresponds to the first passage of the spread at zero, coherently with the above description).

Strategy 1: plain vanilla (PV). This first strategy is a benchmark in the pairs trading literature (see [?]). According to this rule, the investor should open a position as soon as the spread differs from zero. This strategy implies that the investor exploits every deviation of the assets from their long-run relationship and might be highly profitable. However, this rule involves very frequent trading (since the spread oscillates frequently around zero) and, as shown below, might not be profitable as soon as transaction costs are taken into account.

Formally, assuming there is no open position at $t - 1$, a position is opened at t if $S_t \neq 0$.

Strategy 2: probability interval (ProbI). If the investor prefers avoiding too much trading in order to save on transaction costs, she should open a position only when the spread deviates significantly from zero. One common choice to quantify this deviation is to trade when the spread exceeds the so-called Bollinger band (see, e.g., [?]), which coincides with the 95% probability interval under a normality assumption, where the two moments of the distribution are estimated dynamically over a rolling window of n days. This improves on the related strategy analyzed in the seminal work of [?], where the bands are just assumed to be constant and equal to twice the sample standard deviation. The present ProbI strategy generalizes the strategy analyzed in [?], who consider two different bands associated to two alternating market regimes.

Formally, assuming there is no open position at $t - 1$, a position is opened at time t if $S_t \notin (\hat{\mu}_{t-1-n:t-1} \pm q_\alpha \hat{\sigma}_{t-1-n:t-1})$, where $\hat{\mu}_{n_1:n_2}$ (resp. $\hat{\sigma}_{n_1:n_2}$) is the sample mean (resp. standard deviation) estimated using the datapoints from n_1 to n_2 and q_α is the α -quantile of the standard normal distribution. In our empirical analysis we use the 0.975th quantile. This strategy is equivalent to the one based on the z -score (considered for instance in [?]), defined as $z_t := \frac{S_t - \hat{\mu}_{t-1-n:t-1}}{\hat{\sigma}_{t-1-n:t-1}}$, that prescribes to open a position at t if $z_t \notin (-q_\alpha, +q_\alpha)$.

Strategy 3: prediction interval (PredI). By exploiting our stochastic model of Section 2, we can improve on the previous strategy by adopting a forward-looking approach, inspired by [?]. According to the PredI rule, the interval the investor should consider is not the backward-looking confidence interval introduced in strategy ProbI, but rather the prediction interval where the moments are computed according to the stochastic model of Section 2.1.

Formally, assuming there is no open position at $t - 1$, a position is opened at time t if $S_t \notin (\mathbb{E}[S_t | \mathcal{F}_{t-1}^y] \pm q_\alpha \sqrt{\text{Var}[S_t | \mathcal{F}_{t-1}^y]})$, where $\mathbb{E}[S_t | \mathcal{F}_{t-1}^y]$ is the one step-ahead forecast of S_t and $\text{Var}[S_t | \mathcal{F}_{t-1}^y]$ its variance, both computed by relying on the filtering algorithm described in Section 2.2 on the basis of the information generated by spread process y itself. More specifically,

$$\mathbb{E}[S_t | \mathcal{F}_{t-1}^y] = \hat{\gamma}^{(t-1)}(\hat{\mathbf{X}}_{t-1}) + \hat{\alpha}^{(t-1)}(\hat{\mathbf{X}}_{t-1})S_{t-1} \quad \text{and} \quad \text{Var}[S_t | \mathcal{F}_{t-1}^y] = (\hat{\eta}^{(t-1)}(\hat{\mathbf{X}}_{t-1}))^2.$$

Observe that these quantities depend on the filtered estimate of the latent Markov chain \mathbf{X} . Similarly to the ProbI strategy described above, in this strategy we use the 0.975th quantile.

Strategy 4: realized increment (RI). As suggested by [?], another way to avoid too much trading and save on transaction costs is to look for increments of the spread that are significantly “larger than usual”. According to this strategy, the investor has to first compute the time series of the spread increments, that we denote by $x = (x_t)_{t \in \mathbb{N}}$ with $x_t := S_t/S_{t-1} - 1$. Then, she should open a position at time t if the increment x_t is significantly larger than the previous ones. A standard way to formalize this is to rely on two empirical quantiles.

Formally, assuming there is no open position at $t-1$, a position is opened at t if $x_t \notin (q_{\underline{\alpha}, x}, q_{\bar{\alpha}, x})$ with $\underline{\alpha} < \bar{\alpha}$ and where $q_{\alpha, x}$ is the empirical quantile of order α of the spread increment x . In our analysis we consider the $\underline{\alpha} = 0.025^{\text{th}}$ and the $\bar{\alpha} = 0.975^{\text{th}}$ quantiles.

Strategy 5: predicted increment (PI). By exploiting the stochastic model of Section 2, we can improve on strategy RI described above. More specifically, the investor can compute the series $\hat{x} = (\hat{x}_t)_{t \in \mathbb{N}}$ of predicted spread increments, with $\hat{x}_t := \mathbb{E}[S_{t+1} | \mathcal{F}_t^y] / S_t - 1$, and trade whenever the predicted increment lies outside a given interval.

Formally, assuming there is no open position at $t-1$, a position is opened at time t if $\hat{x}_t \notin (q_{\underline{\alpha}, \hat{x}}, q_{\bar{\alpha}, \hat{x}})$. In our analysis we consider the $\underline{\alpha} = 0.025^{\text{th}}$ and the $\bar{\alpha} = 0.975^{\text{th}}$ quantiles.

Finally, we shall also consider two passive strategies that do not incur into transaction costs: a buy-and-hold position on the S&P500 index (S&P strategy), which will be used as a generic benchmark, and a buy-and-hold position on the Invesco DB Oil Fund⁴ (ETF strategy), which is one of the most liquid ETFs for crude oil futures markets and represents a simple alternative for an investor willing to invest in the crude oil futures market.

Remark 3.1 (Alternative statistical arbitrage strategies). Other statistical arbitrage strategies inspired by pairs trading proposed in the literature involve: moving-average trading strategies based on the difference between a short and a long moving average for the spread (see [?]); strategies based on first-passage times when the spread is modelled as a standard Ornstein-Uhlenbeck process (see [?] and [?]); strategies constructed by relying on a machine learning approach that compares possible investment strategies on a training sample (see [?]).

3.2. Performance measurement. As pointed out in [?], computing returns for trading strategies based on the concept of pairs trading is non-trivial due to several factors that complicate the calculation and interpretation of performance metrics. First of all, there are days in which a trading position is open and days in which there is no open position. Moreover, a successfully executed trade delivers a positive cashflow when opened and a non-negative cashflow when closed, thus preventing the computation of a standard linear return. To overcome these issues, it is common to rely on the daily mark-to-market profit & loss indicator.

Let us assume that the strategy is applied over a time period spanning n days. Following [?], for each day $t = 1, \dots, n$ we compute a daily return r_t in the following way:

- if there is no open position at t , then $r_t := 0$;
- if there is an open position at t , then

$$(3.1) \quad r_t := S_t \frac{S_t - S_{t-1}}{V_t^S} - c |S_t - S_{t-1}|,$$

⁴See <https://www.invesco.com/us/financial-products/etfs/product-detail?audienceType=Investor&ticker=DBO>. Numerical experiments show that different alternatives, like the United States Oil Fund ETF or the WisdomTree Crude Oil ETF, are characterized by almost identical performances.

where $V_t^S := |\lambda^0| + \sum_{i=B,S,W} |\lambda^i| F_t^i$ represents the total market exposure of the portfolio and c accounts for proportional transaction costs, as explained below.

The overall performance of a given strategy is then evaluated by computing

$$(3.2) \quad R := \prod_{t=1}^n (1 + r_t) - 1,$$

which can be interpreted as the return over a time period spanning n days. As in our empirical analysis we will consider time periods of different lengths, we shall always report the returns in (3.2) in annual terms: following the usual convention, this amounts to multiply R by $250/n$.

When evaluating the performance of statistical arbitrage strategies, transaction costs can play a significant role, as discussed in [?]. Indeed, these strategies typically involve frequent trading and possibly considerable margins to be posted. Following a common approach in the literature, we take into account these market frictions by introducing in (3.1) the parameter c representing proportional transaction costs. This parameter is however difficult to estimate. Considering the literature on pairs trading on USD-denominated crude oil futures, we found a minimum value of $c = 20\text{bps}$ in [?] and a maximum value of $c = 60\text{bps}$ in [?]. In the present work, we consider trading strategies that include the Shanghai futures, which is denominated in CNY and therefore incurs into currency exchange costs. When including the Shanghai futures in our statistical arbitrage strategies, we assume $c = 80\text{bps}$. This generates a significant amount of transaction costs, which will therefore lead to rather conservative performance measures for our trading strategies.

Unlike pure arbitrage opportunities, statistical arbitrage strategies are not exempt of financial risk. For this reason, we shall also consider the Sharpe ratio, a widely used risk-adjusted performance measure:

$$(3.3) \quad SR := \frac{\frac{1}{n} \sum_{t=1}^n r_t}{\sqrt{\frac{1}{n} \sum_{t=1}^n \left(r_t - \frac{1}{n} \sum_{v=1}^n r_v \right)^2}}.$$

For the sake of comparability, we shall always express the Sharpe Ratio of a given trading strategy in annual terms. In Section 4.2.1, we will perform an additional analysis by also computing the Value-at-Risk of the different strategies introduced in Section 3.1.

4. EMPIRICAL ANALYSIS

This section is divided into four subsections. In Section 4.1, we perform the cointegration analysis among the three futures prices over a fixed time period. In Section 4.2, we evaluate and compare the performance of the statistical arbitrage strategies introduced in Section 3.1. In Section 4.3, we test our strategies with respect to different choices of the futures contracts, replacing the Shanghai futures with the Dubai futures. Finally, in Section 4.4, we verify the robustness of our findings by testing the statistical arbitrage strategies with respect to different levels of transaction costs and over different time periods.

4.1. Cointegration analysis, filtering and parameter estimation.

4.1.1. Data description. We consider daily⁵ and weekly futures prices at one month maturity for the Brent, the WTI and the Shanghai futures, the latter converted from CNY to USD. While the time series for the Brent and the WTI start in the eighties, the Shanghai has been trading

⁵Statistical arbitrage opportunities arise also intraday. See for instance [?] for an analysis of this kind of opportunities in the ETFs market.

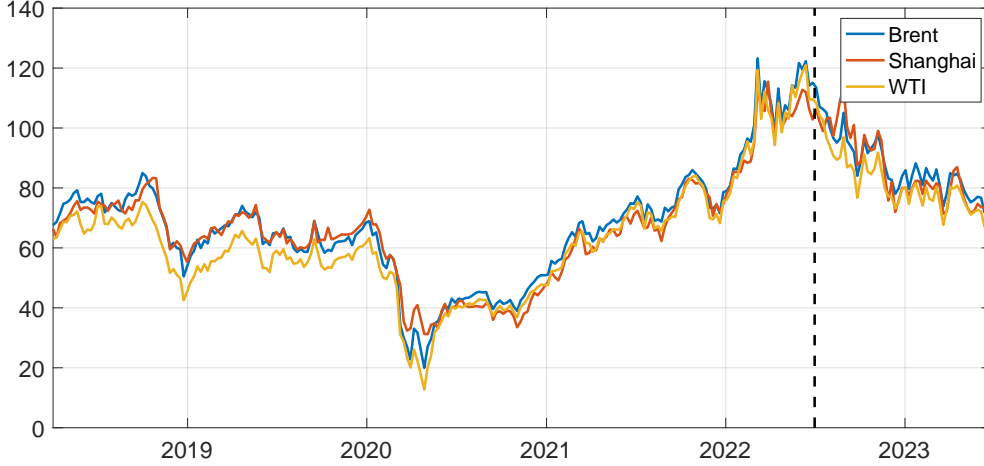


FIGURE 1. Weekly futures prices of the three contracts. The black dashed line corresponds to 07/01/2022, which separates the training sample from the test sample.

	Brent	Shanghai	WTI
ADF	0.9434	0.8507	0.9422
PP	0.8790	0.8386	0.8711
bP	0.9548	0.9402	0.9416

TABLE 1. P-values of the Augmented Dickey-Fuller (ADF), the Phillips-Perron (PP) and the breakpoint Perron (bP) tests. The number of lag length for the ADF and the bP is chosen according to the Schwarz IC.

only since March 2018. Therefore, our dataset spans from $t_0 = 03/26/2018$ to $T = 06/30/2023$, including 1374 daily observations and 274 weekly ones. The weekly futures prices are displayed in Figure 1. We split the full dataset into a *training sample* and a *test sample*. We label by t_B the first date of the test sample, which in our analysis is set at 07/01/2022, represented by a black dashed line in Figure 1. Therefore, the test sample includes a year of observations, corresponding to 261 (resp. 52) daily (resp. weekly) observations.

4.1.2. Unit roots, VAR and cointegration analysis. We perform a cointegration analysis based on weekly data, following the usual steps of cointegration analysis (see, e.g., [?, Chapter 4]). The choice of using weekly data is typical in the literature as daily data tend to be more volatile and noisy due to several factors such as intraday trading, news releases, and other short-term fluctuations. In the Supplementary Materials, we report the results of the cointegration analysis on daily data: while our main findings are not affected by the choice of weekly or daily data, it turns out that the performances of our statistical arbitrage strategies are superior when weekly data are used for the cointegration analysis.

Before assessing the presence of one or more cointegrating relationships among the three futures prices, we test whether each of them is integrated of some order. To this effect, we run standard unit root/stationarity tests on each of the three series individually, running the ADF and the PP tests ([?], [?]) for the presence of a unit root. Moreover, we account for possible structural breaks at an unknown time by running also the breakpoint Perron unit root test ([?]). The p-values of these tests are reported in Table 1. We find a strong evidence that the three series contain (at least) a unit root. The same tests on the first differences of the three series

r	h	Trace test stat.	Crit. val.	pValue
0	1	36.107	35.193	0.039
1	0	10.648	20.262	0.603
2	0	1.250	9.164	0.915

SBIC($r = 1$): 12.9533

TABLE 2. Results of [?] trace test. h is the rejection decision of the trace test with null hypothesis “there exist less than or equal to r cointegrating relationships”.

deliver p-values all lower or equal to 1%, indicating that the series contain only one unit root. Therefore, we can conclude that the three series are integrated of order one.

Given the similarities among the three crude oil futures contracts, it is natural to study whether the stochastic trend found in the three series is common. Among the two main approaches to cointegration, the one of [?] and the one of [?] and [?], we opt for the latter. Indeed, the Engle and Granger approach would require to choose a priori a reference futures contract among the three under consideration and there is no objective way to do so. In order to assess any cointegrating relationship by means of the Johansen procedure, we first formulate a vector autoregressive model of order p (VAR(p) henceforth). We choose p by minimizing the Schwarz IC, which is known to deliver the most parsimonious specification. On our test sample, we obtain that the optimal number of lags p is equal to two (this result is quite stable even when considering different test samples, namely when changing t_0 and/or t_B). The resulting (reduced-form) VAR(2) can be written as

$$\mathbf{F}_t = \mathbf{a}_0 + \mathbf{A}_1 \mathbf{F}_{t-1} + \mathbf{A}_2 \mathbf{F}_{t-2} + \mathbf{u}_t$$

where $\mathbf{F}_t = (F_t^B, F_t^S, F_t^W)$ are the three variables of interest, $\mathbf{a}_0 \in \mathbb{R}^3$, $\mathbf{A}_i \in \mathbb{R}^{3 \times 3}$, $i = 1, 2$, are the parameters of the model and \mathbf{u}_t is a three-dimensional white noise process with covariance matrix $\Sigma \in \mathbb{R}^{3 \times 3}$. The VAR(2) model is estimated by ordinary least squares and the resulting point estimates and standard errors are given by

$$\begin{aligned} \begin{bmatrix} F_t^B \\ F_t^S \\ F_t^W \end{bmatrix} &= \begin{bmatrix} 1.546 \\ (1.095) \\ 1.111 \\ (0.883) \\ 1.353 \\ (1.093) \end{bmatrix} + \begin{bmatrix} 0.614^{**} & 0.088 & 0.147 \\ (0.249) & (0.125) & (0.234) \\ 0.510^{**} & 0.555^{***} & -0.100 \\ (0.201) & (0.101) & (0.189) \\ -0.221 & 0.111 & 0.968^{***} \\ (0.249) & (0.125) & (0.233) \end{bmatrix} \begin{bmatrix} F_{t-1}^B \\ F_{t-1}^S \\ F_{t-1}^W \end{bmatrix} \\ &+ \begin{bmatrix} 0.266 & -0.157 & 0.033 \\ (0.258) & (0.113) & (0.238) \\ -0.221 & 0.157^* & 0.078 \\ (0.208) & (0.091) & (0.192) \\ 0.242 & -0.214^* & 0.100 \\ (0.257) & (0.112) & (0.237) \end{bmatrix} \begin{bmatrix} F_{t-2}^B \\ F_{t-2}^S \\ F_{t-2}^W \end{bmatrix} + \begin{bmatrix} u_t^B \\ u_t^S \\ u_t^W \end{bmatrix} \end{aligned}$$

where ***, ** and * represent, respectively, a statistical significance at the 1%, 5% and 10% level. Inspecting the roots of the characteristic equation, this VAR(2) appears to satisfy the stability condition. We can now perform the cointegration test. We adopt the trace test of [?] and allow for a constant in the cointegrating relationship. Looking at the results reported in Table 2, the test indicates the presence of only one cointegrating relationship. Moreover, in our dataset we find that this result is robust also when considering different time windows. We can therefore estimate the following vector error correction model (VECM henceforth):

$$\Delta \mathbf{F}_t = \boldsymbol{\pi}_0 + \boldsymbol{\Pi}_0 \mathbf{F}_{t-1} + \boldsymbol{\Pi}_1 \Delta \mathbf{F}_{t-1} + \boldsymbol{\Pi}_2 \Delta \mathbf{F}_{t-2} + \boldsymbol{\varepsilon}_t$$

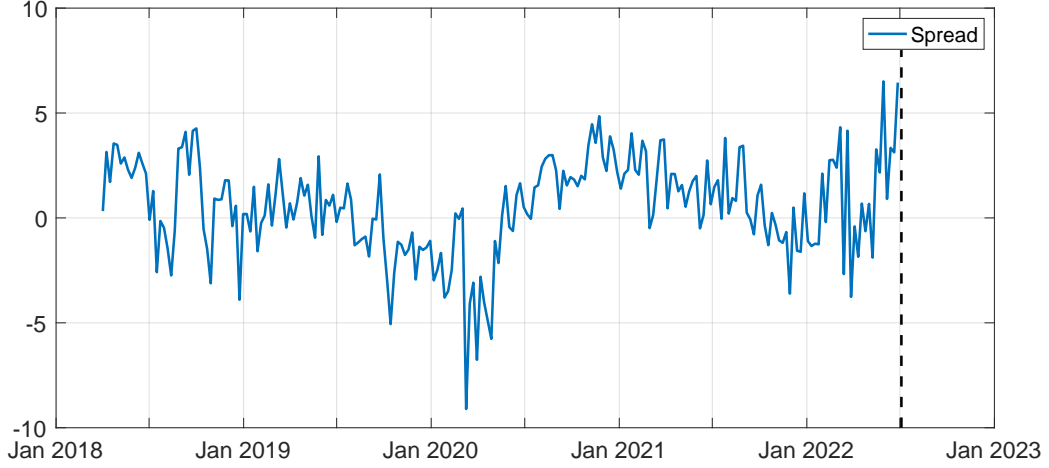


FIGURE 2. Resulting spread process within the test sample.

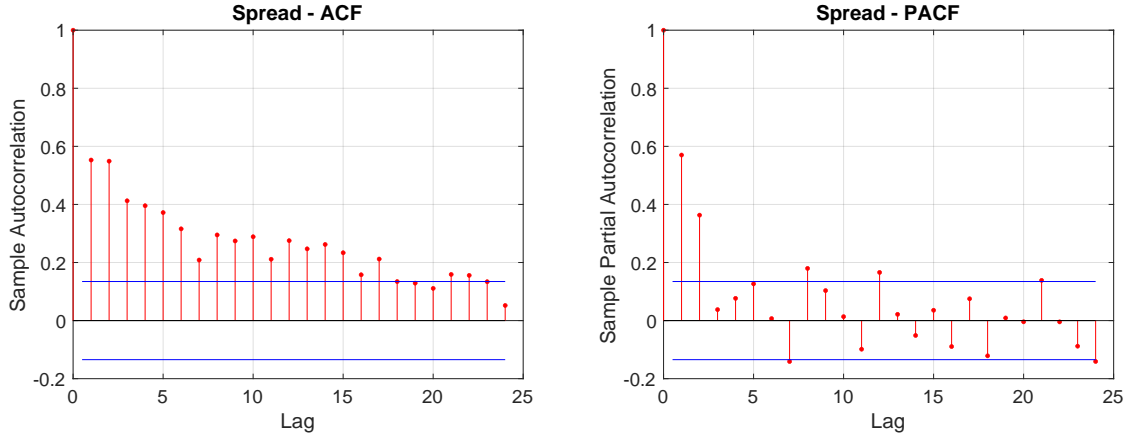


FIGURE 3. ACF and PACF of the spread process over the training sample, weekly observations.

where Δ is the first difference operator and $\boldsymbol{\pi}_0 \in \mathbb{R}^3$, $\boldsymbol{\Pi}_i \in \mathbb{R}^{3 \times 3}$, $i = 0, 1, 2$, $c \in \mathbb{R}$ are the parameters of the model and $\boldsymbol{\varepsilon}_t$ is a three-dimensional white noise process with covariance matrix $\boldsymbol{\Sigma}_u \in \mathbb{R}^{3 \times 3}$.

Since we cannot reject that $\text{rank}[\boldsymbol{\Pi}_0] = 1$, the matrix $\boldsymbol{\Pi}_0$ can be decomposed as $\boldsymbol{\Pi}_0 = \boldsymbol{\alpha}\boldsymbol{\beta}^T$ with $\boldsymbol{\beta} \in \mathbb{R}^3$. Rewriting $\boldsymbol{\pi}_0$ as $\boldsymbol{\pi}_0 = \boldsymbol{\alpha}c_0$, with $c_0 \in \mathbb{R}$, we can derive the expression of the resulting cointegration relationship, $c_0 + \boldsymbol{\beta}^T \mathbf{F}_t$, which is our spread process S , and the adjustment coefficients $\boldsymbol{\alpha}$ that measure the speed of convergence of each series to the long-run relationship. Therefore, in our test sample the spread process results to be given by

$$(4.1) \quad S_t = F_t^B - 0.6982F_t^S - 0.3402F_t^W + 0.4322$$

and it is plotted in Figure 2. As can be seen from this figure, the spread process exhibits a stationary behavior. Coherently, the ADF and PP tests reject the null hypothesis of the presence of a unit root while the KPSS test ([?]) cannot reject the null hypothesis of stationarity of the series. Moreover, as can be seen from Figure 3, both the ACF and the PACF of S decline to zero. In particular, only the first two lags of the PACF seem to be statistically different from zero. This indicates some degree of mean-reversion of S that empirically justifies modelling S by means of the stochastic model introduced in Section 2.1.

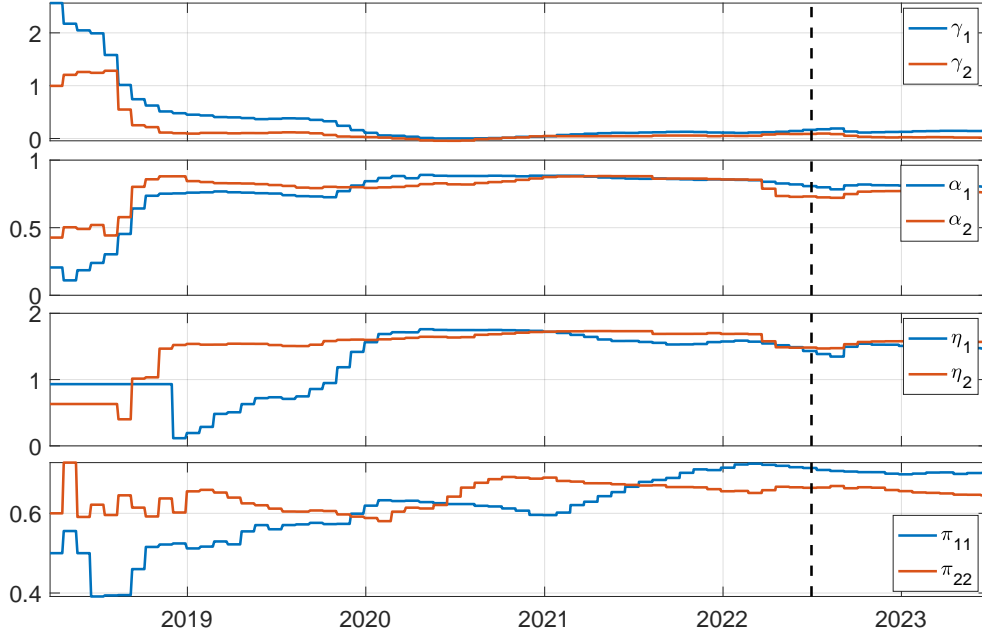


FIGURE 4. Recursively updated estimates of γ_i , α_i , η_i and π_{ii} , $i = 1, 2$, for the $N = 2$ OU-HMM.

The estimated adjustment coefficients of the VECM are $\boldsymbol{\alpha} = [0.0640 \quad 0.4226 \quad 0.0684]^\top$. It is interesting to observe that the Shanghai futures price realigns to the long-run equilibrium much faster than the other two futures prices. As a high speed of adjustment in one or more of the portfolio constituents is a desirable property when constructing statistical arbitrage strategies, this provides a preliminary indication of the potential profitability of including the Shanghai futures in the context of crude oil futures portfolios.

4.1.3. Filtering the spread. We now estimate the parameters of the OU-HMM for S . We first determine the most likely number N of the states of the latent Markov chain \mathbf{X} ; we then compute daily filtered estimates of \mathbf{X} ; finally, we estimate the model parameters $\boldsymbol{\gamma}$, $\boldsymbol{\alpha}$, $\boldsymbol{\eta}$ in (2.3) and the transition matrix $\boldsymbol{\Pi}$ by means of the filter-based EM algorithm described in Section 2.2. We implement the filtering and parameter estimation procedure on daily data. The choice of daily data is motivated by two reasons: first, we want to rely on a large dataset for the estimation of the parameters of the spread process, in order to capture its short-term variations; second, we want to possibly implement trading strategies on a daily basis rather than on a weekly basis.

The daily spread process is determined by using the weights reported in (4.1). We estimate the whole model for $N \in \{1, 2, 3\}$ and compute the information criteria and the mean square error at the end of the training sample. Although most of the times there is complete agreement among the different information criteria on the optimal value of N , we follow the Schwarz IC. According to this criterion, we find that in our training sample the best model entails $N = 2$ states of the Markov chain \mathbf{X} .

Figure 4 illustrates the time evolution of the filtered estimates of the model parameters $\boldsymbol{\gamma}$, $\boldsymbol{\alpha}$, $\boldsymbol{\eta}$ and of the probabilities π_{ii} , $i = 1, 2$, of the Markov chain \mathbf{X} to remain in its current state. Due to the well-known issue of slow convergence of the EM algorithm, the estimates turn out to be unstable at the beginning of the training sample. Afterwards, they stabilize and only major changes in the underlying observations have an impact on the estimates. For the sake of completeness, the parameter estimates at the end of the training sample are reported in Table 3. As we can see, the main feature that differentiates the two regimes is the value of γ : the

	state 1	state 2		state 1	state 2
γ	0.1632	0.0869	β	0.8490	0.3233
α	0.8077	0.7313	a	53.3830	78.2361
η	1.4312	1.4832	ξ	25.0833	27.2027
π_{11}	0.7138		π_{22}	0.6640	

TABLE 3. Point estimates of the functions of the OU-HMM (both in discrete and continuous time) at the end of the training sample.

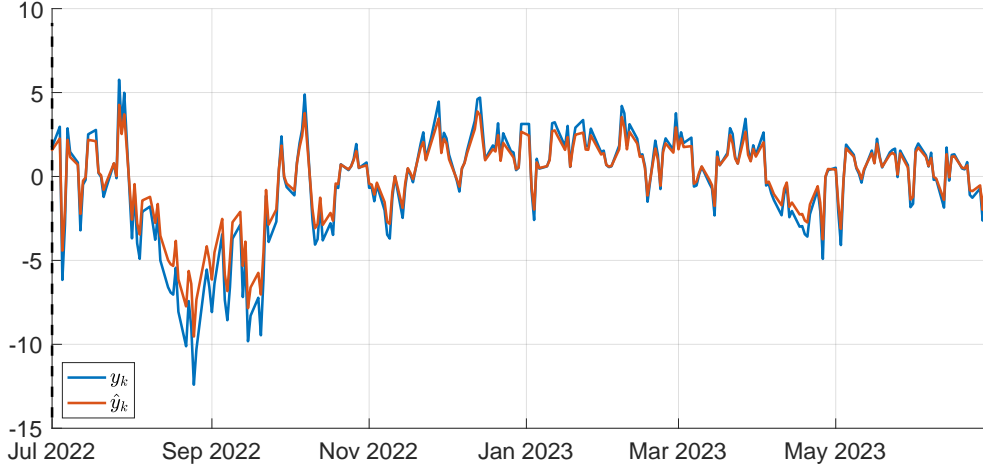


FIGURE 5. One-step ahead forecasts and actual values of y across the test sample.

two regimes display almost the same level of persistence α , the same level of volatility η but a different mean level γ . This difference turns out to be even more striking in the other training samples considered below and most of the times we find $\gamma_1 > 0$ and $\gamma_2 < 0$.

Figure 5 displays the one-step ahead forecast of S along with the realized value across the test sample. As can be seen from this figure, the filtering algorithm produces fairly good forecasts of the realizations of the spread.

4.2. Testing the strategies. We now analyze over the test sample (from $t_B = 07/01/2022$ until $T = 06/30/2023$) the five different statistical arbitrage strategies described in Section 3.1: the plain Vanilla (PV), the probability interval (ProbI), the prediction interval (PredI), the realized increment (RI), the predicted increment (PI), along with the buy-and-hold S&P500 and the crude oil ETF strategies. For each strategy we compute the opening/closing signals, the annualized return according to (3.2) and the annualized Sharpe ratio according to (3.3).

Figure 6 illustrates how the signals differ across the five statistical arbitrage strategies. We immediately notice that the number of trades over the test sample varies significantly across the different strategies. Excluding the PV strategy that entails always an open position as soon as $S_t \neq 0$, we document a minimum of five trades with the ProbI strategy and a maximum of twenty-nine trades with the PredI strategy. Moreover, also the length of the open positions varies considerably: indeed, we generate positions that are opened on a given day and closed on the following day together with positions that remain open for several months.

Table 4 summarizes the return (R) and Sharpe ratio (SR), as described in Section 3.2, assuming $c = 80\text{bps}$. As mentioned in Section 3.2, this relatively high level of transaction costs yields a conservative assessment of the performance of our statistical arbitrage strategies involving the

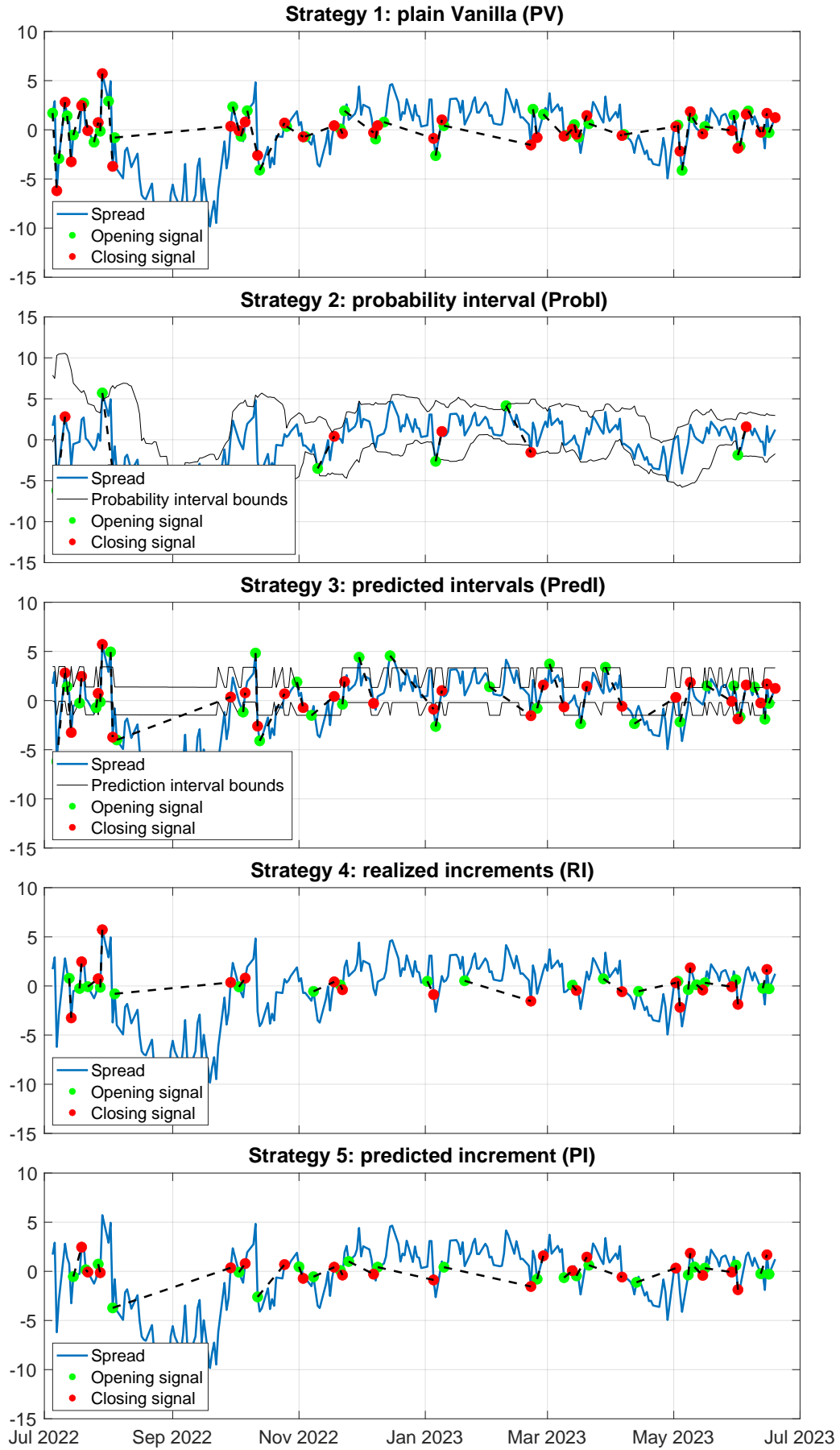


FIGURE 6. Opening/closing signals of the statistical arbitrage strategies described in Section 3.1 over the test sample of Section 4.1.

	PV	ProbI	PredI	RI	PI	S&P	ETF
R	13.03%	56.37%	72.77%	-1.43%	22.41%	16.43%	-25.46%
SR	0.6082	1.0849	1.0108	0.4440	0.6836	0.8868	-0.6299

TABLE 4. Annualized performances with $c = 80\text{bps}$ over the test sample of Section 4.1 including the Brent, the Shanghai and the WTI futures contracts.

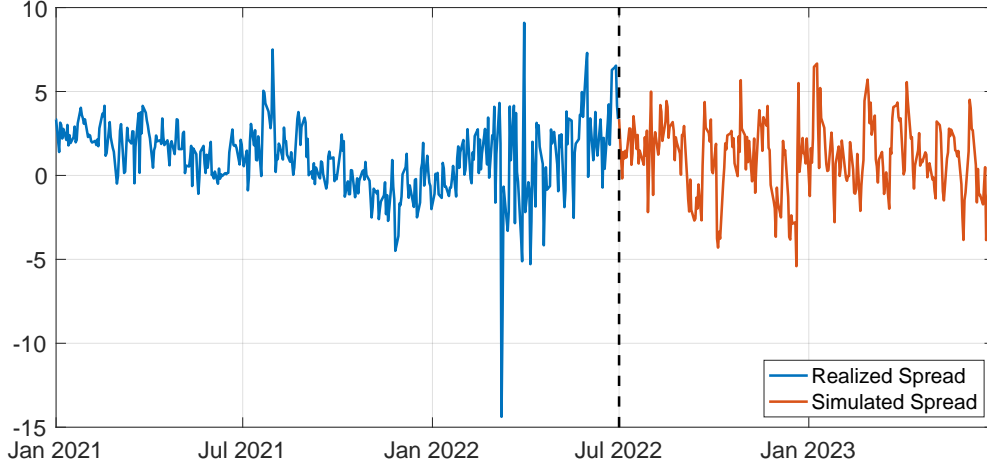


FIGURE 7. A simulated out-of-sample trajectory of the spread.

Shanghai futures. First of all, we notice that the ETF on the crude oil futures market performs poorly on the test sample. This is coherent with the global decline of crude oil futures prices over the test sample which is clear from Figure 1. Moving to statistical arbitrage strategies, we find that only the PV and RI strategies deliver a return lower than the S&P strategy, which entails no transaction costs. On the contrary, the ProbI, PredI and PI strategies outperform the S&P strategy and deliver significant returns, overcoming the considerable amount of transaction costs assumed in our analysis. In particular, it turns out that the forward-looking strategies PredI and PI that are based on the stochastic model introduced in Section 2 outperform the simpler ProbI and RI strategies that rely only on past observations of the spread. We can therefore conclude that our OU-HMM model seems to have promising applications for optimal investment in international crude oil futures markets.

4.2.1. Risk analysis. Statistical arbitrage strategies might involve a considerable financial risk. In particular, when opening a position, the investor does not know when the futures prices will realign or whether convergence will ever be reached. As a consequence, the investor might find herself stuck in a costly position to maintain (due to margin calls) and that does not generate any profit for a prolonged period of time. In this section, we assess the riskiness of the statistical arbitrage strategies by means of a Monte Carlo analysis.

First of all, we compute the out-of-sample daily Value-at-Risk (VaR henceforth) of the strategies described in Section 3.1. Moreover, we exploit the simulations that are required for VaR estimation in order to derive the empirical distribution of the annualized returns of our strategies. This is done by implementing the following successive steps:

- (1) we estimate the cointegration relationship over the training sample;
- (2) we filter the resulting spread over the training sample following Section 4.1.3;

	PV	Probl	PredI	RI	PI	S&P	ETF
$VaR_{99\%}$	-10.21%	-10.86%	-10.16%	-7.93%	-7.62%	-2.80%	-5.29%
$VaR_{95\%}$	-5.88%	-5.49%	-5.80%	-3.66%	-3.69%	-1.72%	-3.80%
$VaR_{90\%}$	-4.04%	-3.35%	-3.87%	-1.94%	-2.12%	-1.29%	-3.13%

TABLE 5. Monte Carlo estimates of the daily VaRs of daily returns over the test sample of Section 4.1 including the Brent, the Shanghai and the WTI futures contract ($NSim = 1000$; the average t-statistics is equal to almost 6).

- (3) at the breaking date t_B we retrieve the optimal estimated number of states N of the Markov chain and the related point estimates of the parameters of our OU-HMM model;
- (4) for $i = 1, \dots, NSim$:
 - we simulate over the test sample (i.e. from t_B to T) a trajectory of the latent Markov chain \mathbf{X} with the optimal N found before;
 - we simulate over the test sample the spread process following (2.3) and the realizations of \mathbf{X} simulated at the previous step using the parameters obtained at the end of the training sample. Figure 7 shows a simulated trajectory of the spread;
 - we compute the series of the returns according to (3.1) of the different statistical arbitrage strategies described in Section 3.1;
 - we compute the daily VaR at the confidence levels 1%, 5% and 10%;
 - we compute the overall performance of the strategies in terms of annualized return (3.2) and Sharpe ratio (3.3);
- (5) we average out the VaRs obtained along all the $NSim$ trajectories;
- (6) we compute the Kernel Density Estimator (KDE henceforth) of the annualized returns obtained along all the $NSim$ trajectories.

Table 5 displays the Monte Carlo estimates of the daily VaRs at the usual confidence levels. As expected, the attractive performances of statistical arbitrage opportunities involving the Shanghai futures reported in Table 4 are mitigated by a considerable level of risk, if compared to the simple S&P strategy. This implies that an arbitrageur willing to engage in statistical arbitrage strategies involving the Shanghai futures has to be ready to face possibly severe drops of the market value of her portfolio which may call for extra margins to be posted.

Figure 8 displays the Monte Carlo-based KDEs of the annual returns of the five strategies over the test sample. As we can see, all densities are positively skewed, with a sizeable amount of probability mass associated to positive returns. This provides evidence that statistical arbitrage strategies that are designed by exploiting the OU-HMM model introduced in Section 2 yield profitable investment opportunities.

4.3. Choice of the underlying futures contracts. In order to assess the relevance of the results reported in the previous subsection, we test the same statistical arbitrage strategies using different choices of futures contracts. First, we follow the traditional approach to pairs trading by using strategies that involve only two futures contracts instead of three. Then, we consider an alternative triplet of securities, replacing the recently introduced Shanghai futures with the Dubai crude oil futures, a well-established benchmark for crude oil.

The results of this analysis are reported in Table 6. For comparison purposes, the first row replicates the data from Table 4, while the performances of the benchmark passive strategies, S&P (R: 16.43%, SR: 0.8868) and ETF (R: -25.46%, SR: -0.6299), are omitted. Transaction costs are set at $c = 80\text{bps}$ when trading the Shanghai futures and reduced to $c = 20\text{bps}$ when only

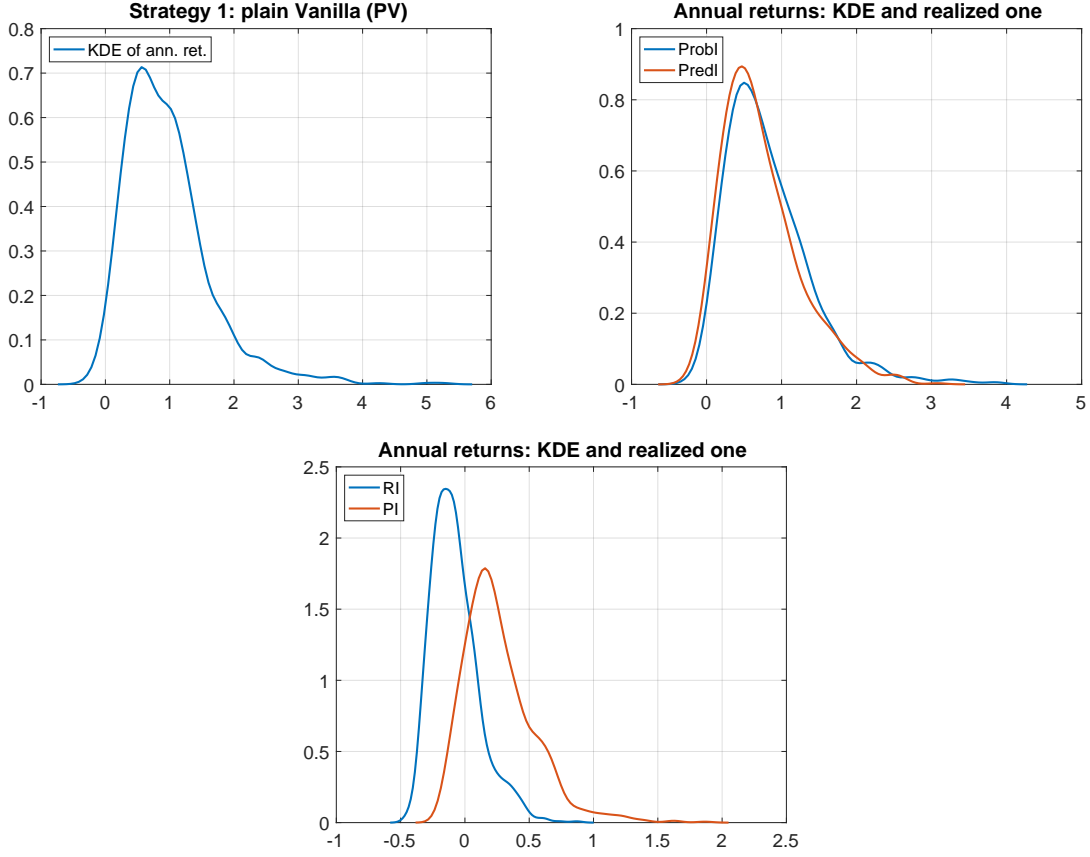


FIGURE 8. Monte Carlo-based KDEs of annual returns over the test sample of Section 4.1 including the Brent, the Shanghai and the WTI futures contract ($N\text{Sim} = 1000$).

well established crude oil futures (Brent, WTI, and Dubai) are used. As discussed in Subsection 3.2, $c = 80\text{bps}$ is likely an overestimate. However, we prefer to maintain this conservative figure to account for any potential friction an investor might encounter when trading the recently introduced Shanghai futures. In contrast, $c = 20\text{bps}$ represents a lower bound of transaction costs, which is more plausible when trading well-established futures contracts.

As shown in Table 6, all the proposed statistical arbitrage strategies, except for the RI strategy, perform best when trading the Brent, Shanghai, and WTI futures, compared to any other combination involving these three or the Dubai futures, and despite the much higher transaction costs considered for the Shanghai futures. The second-best performing set of futures to trade is the simple Brent-WTI pair, which delivers positive returns for all strategies. While the triplet Brent-Shanghai-WTI is the most profitable, when replacing the recently introduced Shanghai futures with the Dubai one, the performance of our statistical arbitrage strategies deteriorate, despite the lower transaction costs. This might be explained by the fact that, as soon as the underlying assets become widespread, statistical arbitrage opportunities tend to disappear, as already noted in the literature (see, e.g., [?]).

Finally, it is noteworthy that, over this specific training period, the WTI does not appear to cointegrate with neither the Shanghai nor the Dubai. Although unusual, this can happen occasionally, as can also be seen from Figure 10, and might indicate some persistent deviation of the WTI from the other crude oil futures.

4.4. Robustness analysis. To assess the robustness of our findings, we now systematically repeat the analysis carried out in the previous sections changing the transaction costs parameter

	c	PV	ProbI	PredI	RI	PI
Brent - Shanghai - WTI						
R	80bps	13.03%	56.37%	72.77%	-1.43%	22.41%
SR	80bps	0.6082	1.0849	1.0108	0.444	0.6836
Brent - Shanghai						
R	80bps	-59.05%	36.29%	-51.21%	-24.11%	-50.73%
SR	80bps	0.003	0.8127	0.1319	-1.0759	0.1704
Shanghai - WTI						
No statistical evidence of cointegration						
Brent - WTI						
R	20bps	11.39%	10.39%	10.47%	4.88%	11.4%
SR	20bps	0.8891	0.8314	0.8278	0.5404	0.8895
Brent - WTI - Dubai						
R	20bps	6.45%	7.21%	7.22%	0.00%	-0.60%
SR	20bps	0.6195	0.7115	0.6852	0.0363	-0.0299
Brent - Dubai						
R	20bps	1.24%	5.65%	-0.21%	-0.61%	-4.64%
SR	20bps	0.171	0.5978	0.0295	-0.2278	-1.2266
WTI - Dubai						
No statistical evidence of cointegration						

TABLE 6. Annualized performances over the test sample including different combinations of the Brent, the Dubai, the Shanghai and the WTI futures contracts.

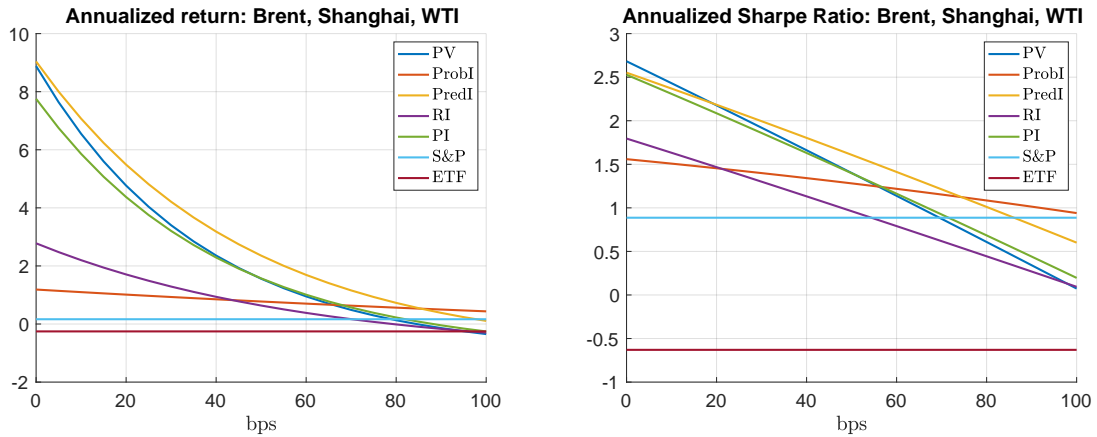


FIGURE 9. Performances of the strategies with respect to c ; $t_0 = 03/26/2018$, $t_B = 07/01/2022$.

c , the starting date t_0 of the sample and the breaking date t_B that divides the training sample from the test one.

4.4.1. *Sensitivity with respect to transaction costs.* Figure 9 displays the performances of the statistical arbitrage strategies as a function of c . Obviously, both the annualized return R and the Sharpe ratio SR are declining in c . The slope of this decline is proportional to the frequency

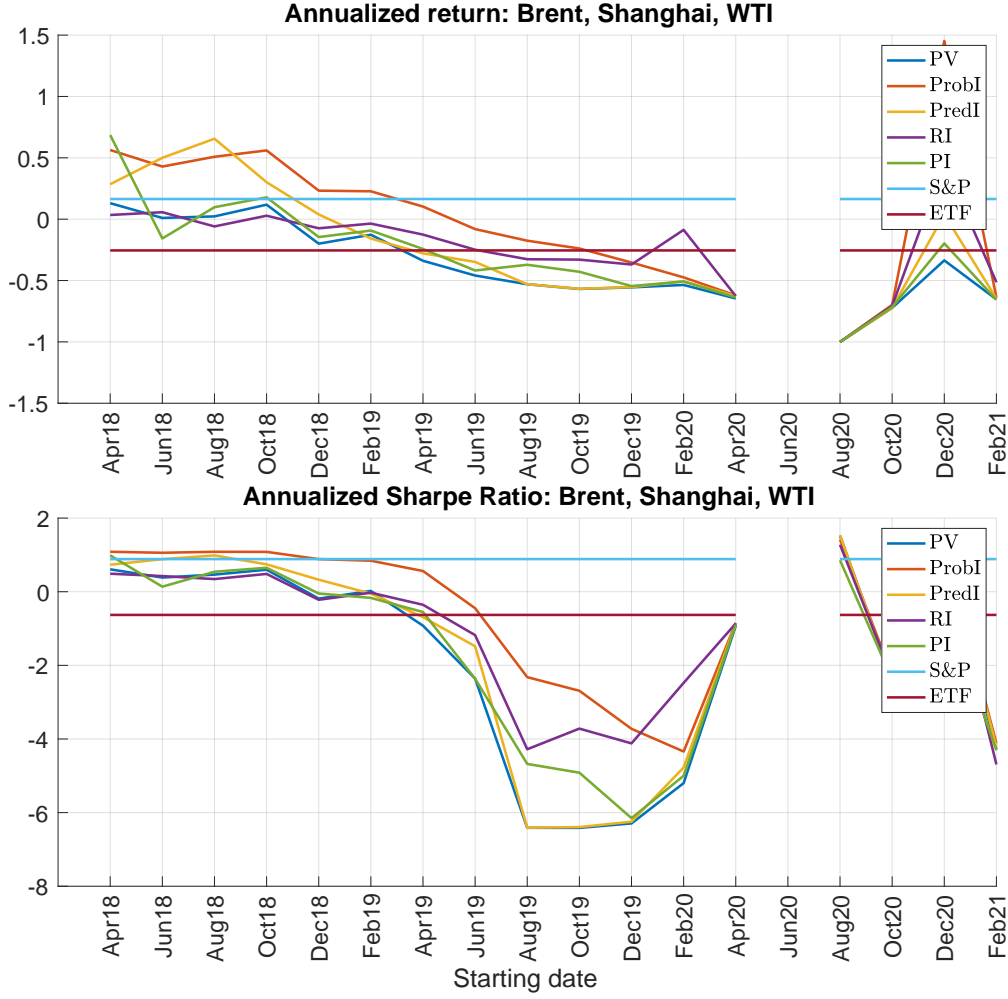


FIGURE 10. Performances of the strategies with respect to t_0 ; $c = 80\text{bps}$, $t_B = 07/01/2022$. Missing datapoints are due to the rejection of cointegration among the futures contract over the related time window.

of opening/closing positions: the performances of strategies PV, PredI and PI that prescribe the opening of several trades (see Figure 6) are the most sensible to c while strategies ProbI and RI are less affected by transaction costs. We find that, over the considered time period, statistical arbitrage strategies that include the Shanghai futures are quite robust with respect to the level of transaction costs. In particular, the benchmark S&P passive strategy becomes preferable only when c approaches 1%. It is also noteworthy that the strategies that make use of the OU-HMM model introduced in Section 2.1, namely the PredI and the PI strategies, turn out to be very profitable for small (but realistic) levels of transaction costs. In our view, this represents a further evidence of the potential advantages of relying on a stochastic model in the design of statistical arbitrage strategies.

4.4.2. Sensitivity with respect to t_0 . Figure 10 depicts the performance of our strategies as a function of the starting date t_0 of the sample. Since the breaking date t_B is fixed, if t_0 moves forward the number of observations in the training sample shrinks. This is expected to worsen the quality of the filter-based estimates derived according to the algorithm described in Section 2.2, due to the availability of a smaller number of observations. As we can see from Figure 10, reducing the training sample weakens the cointegrating relationship among the time series and, as a consequence, lowers the performance of our strategies. This indicates that, in order to be

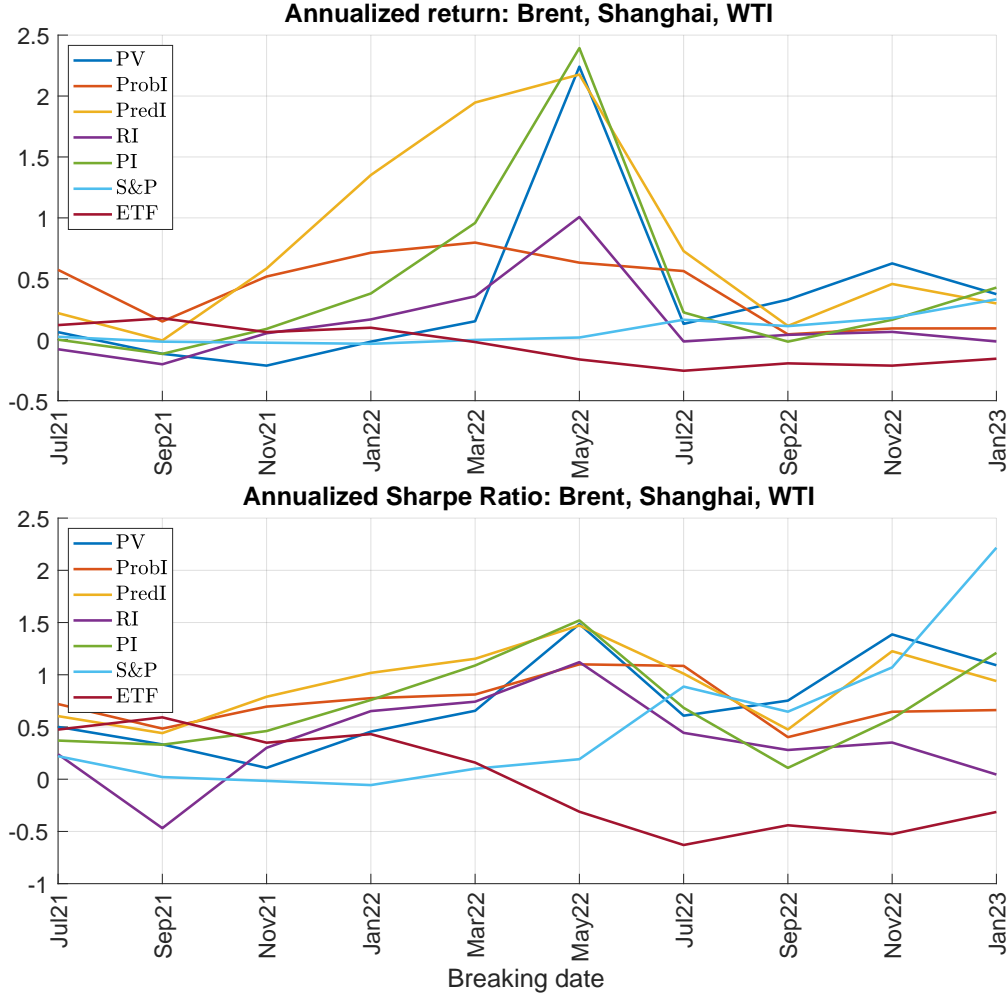


FIGURE 11. Performances of the strategies with respect to t_B ; $c = 80\text{bps}$, $t_0 = 03/26/2018$.

profitable, our statistical arbitrage strategies require a minimum sample size for the model to be accurately estimated. From Figure 10 we can also notice that the dataset is significantly affected by the market turmoil of the COVID-19 pandemics. Given the rather recent introduction of the Shanghai futures, this issue cannot be avoided, since the available dataset is relatively small.

4.4.3. Sensitivity with respect to t_B . Figure 11 shows the performance of our strategies as a function of the breaking date t_B . As t_B moves backward, the training sample shrinks, while the test sample becomes longer. The impact on the performance of statistical arbitrage strategies is therefore twofold. On the one hand, reducing the size of the training sample weakens the reliability of estimated cointegration model. On the other hand, a larger test sample provides more opportunities for profitable trades. In our dataset, a small decline in the performance is registered for t_B before than March-July 2022. Bringing t_B forward has ambiguous effects as well: the cointegration is estimated over a larger training sample but there is less time to take advantage of that. As shown in Figure 11, in our dataset we document a small increase of the performances for t_B after March-July 2022.

5. CONCLUSIONS

In this work, we have investigated statistical arbitrage strategies that generalize pairs trading strategies, involving the two established crude oil futures contracts, the Brent and the WTI,

together with the more recently introduced Shanghai crude oil futures. We have documented that the time series of the three futures prices are cointegrated. In order to dynamically model the resulting cointegration spread, we have proposed a mean-reverting stochastic process with regime switching modulated by an unobservable Markov chain. The model is estimated by relying on a filter-based version of the EM algorithm, thereby ensuring that the model stays dynamically tuned to the market situation. We have considered and analyzed several statistical arbitrage strategies, showing that strategies designed by relying on our stochastic model are remarkably profitable, even under conservative levels of transaction costs. Based on these results, we believe that it would be interesting to evaluate alternative investment strategies based on our stochastic model and study optimal portfolio problems by relying on the techniques of stochastic optimal control under partial information.

Our findings suggest that, despite the well established cointegration among the Brent, the WTI and the Dubai crude oil futures, profitable statistical arbitrages in these three assets seem to have been exhausted. This is not the case for the Shanghai futures, which yields significant investment performances even if subject to a non-negligible level of risk. The introduction of the Shanghai futures is quite recent and, therefore, more extensive empirical analysis will be needed in order to assess the specific features of this security in the context of global financial markets.

REFERENCES

DEPARTMENT OF ECONOMICS, MANAGEMENT AND BUSINESS LAW, UNIVERSITY OF BARI ALDO MORO, ITALY.
E-mail address: `viviana.fanelli@uniba.it`

DEPARTMENT OF MATHEMATICS "TULLIO LEVI - CIVITA", UNIVERSITY OF PADOVA, ITALY.
E-mail address: `fontana@math.unipd.it`

DEPARTMENT OF FINANCE, BOCCONI UNIVERSITY, ITALY.
E-mail address: `rotondi.francesco@unibocconi.it`